

# Investigation of Energetic Ions in a 100-A Hollow Cathode

Benjamin A. Jorns\* Ioannis G. Mikellides† and Dan M. Goebel ‡

*Jet Propulsion Laboratory, California Institute of Technology, Pasadena, CA 91109*

The role of ion acoustic turbulence in the formation of high-energy ion tails in the plume of a 100-A LaB<sub>6</sub> hollow cathode is experimentally and theoretically examined. At fixed flow rate and varying discharge current, single-point measurements of fluctuation intensity in the cathode plume are taken and compared to ion energy measurements. It is shown that for high discharge current the formation of energetic ions is correlated with the amplitude of the ion acoustic turbulence. Two-dimensional maps of background plasma parameters and wave turbulence are made at the highest discharge current investigated, 140 A. A simple, one-dimensional quasilinear model for the interaction of the ion energy distribution with the ion acoustic turbulence is employed, and it is shown that the energy in the measured wave turbulence is sufficiently large to explain the formation of ion tails in the cathode plume. Mitigation techniques for minimizing the amplitude of the turbulence are discussed.

## Nomenclature

$f_i$	Ion distribution function
$c_s$	Ion sound speed
$T_{e,i}$	Species temperature in units of energy
$m_{e,i}$	Species mass
$v_\phi$	Wave phase velocity
$v_{te,ti}$	Species thermal velocity
$v_{di,de}$	Species drift velocity
$M_e$	Electron Mach number
$\nu_{AN}$	Anomalous collision frequency
$\omega_{pe,pi}$	Species plasma frequency
$\lambda_i$	Ion Debye length
$n_{e,i}$	Time-averaged species density
$E_i$	Ion energy
$i_{sat}$	Ion saturation current
$\phi$	Amplitude of fluctuation in plasma potential
$\phi_p$	Time-averaged plasma potential
$\phi_F$	Floating potential
$V_D$	Cathode discharge voltage

---

\*Associate Engineer, Electric Propulsion Group, AIAA member, benjamin.a.jorns@jpl.nasa.gov

†Principal Engineer, Electric Propulsion Group, AIAA Associate Fellow

‡Senior Research Scientist, Thermal and Propulsion Engineering Section, AIAA Fellow

$I_D$	Cathode discharge current
$k$	Wavenumber
$\omega$	Wave frequency
$D_{QL}$	Quasilinear diffusion coefficient

## I. Introduction

The erosion of hollow cathodes at high currents is a major failure mechanism for thrusters that rely on this element for operation.<sup>1,2</sup> This failure can take place in two ways: orifice erosion and sputtering of the cathode keeper face. While both of these process result from ion bombardment, it is only the erosion at the orifice that is currently well-understood and has known techniques for mitigation.<sup>3</sup> Keeper erosion, on the other hand, is still considered anomalous. This is because keeper sputtering results from impact by ions from the cathode plume with energies that far exceed the cathode discharge voltage,<sup>4–11</sup> yet there is no classical reason why such high energy ions should exist. The erosion from these anomalous ions is becoming an increasingly important concern in light of new NASA programs that are calling for higher power electric propulsion missions with extended duration. Indeed, understanding and ultimately mitigating the keeper erosion produced by the anomalous energetic ions in the cathode plume is paramount for enabling these future missions.

With this in mind, there have been a number of attempts to identify the source of high energy ions in the cathode plume.<sup>9,12–16</sup> One particularly promising candidate for this process—especially at high discharge current—is the interaction of the ions with ion acoustic turbulence (IAT). IAT is known to be driven unstable in current-carrying plasmas,<sup>17</sup> and it has been found that even low level plasma fluctuations of this instability can lead to the formation of high energy ion tails.<sup>18,19</sup> Moreover, there is strong evidence that IAT exists in the plumes of high-current cathodes. In early work with high current electric propulsion hollow cathodes (up to 60 A), Friedly and Wilbur<sup>5</sup> observed plasma “noise” in the discharge and considered the ion acoustic instability as the cause of this noise based on the experimental findings of Guyot and Hollenstein<sup>20</sup> for current-carrying plasmas. Later, Mikellides et al.<sup>21</sup> showed by numerical simulation of the plasma inside a hollow cathode operating at 25 A that the electron Mach number, electron temperature, and electron-to-ion temperature ratio were high enough to support the presence of IAT. Mikellides et al.<sup>22</sup> theorized in a subsequent paper that the IAT could lead to anomalous resistivity in the cathode plume—3 to 100 times the classical value. Without this effect, their cathode model could not accurately recreate the time-averaged experimental measurements that had been made by Goebel et al.<sup>23,24</sup> In a recent investigation of a 100-A LaB<sub>6</sub><sup>25</sup> cathode, we experimentally demonstrated with dispersion measurements that IAT does in fact exist in the cathode plume, and through the application of kinetic theory, we showed how its growth can lead to a drag on the electrons. We found that the effective collisionality that resulted from this drag was sufficiently high to explain the anomalous resistivity used in numerical simulations of the same cathode plume.<sup>26</sup>

In light of these theoretical and experimental results, it is clear that the IAT can and does exist in cathode plumes. This is a significant result because it has been shown that for sufficiently large amplitudes, IAT can transfer its energy to plasma ions through collisionless processes such as ion Landau damping.<sup>17,27</sup> This process in turn can lead to the formation of energetic ion tails. For cathode plumes, the question is whether or not the turbulence is strong enough to produce the amount of energy observed in the experimentally-measured ion tails. Friedly and Wilbur concluded this could not be the case for their cathode since their measured fluctuation level was small (< few volts) as compared to the high-energy “ion jets” they observed.<sup>5</sup> However, these authors failed to take into account that the mechanism for energy transfer with IAT does not depend only on wave amplitude but also on the instability growth rate and kinetic energy. This can lead to large heating even if the wave amplitudes are small.<sup>17</sup> Mikellides<sup>16</sup> et al., on the other hand, identified the IAT as a viable candidate to explain the formation of energetic ions in the plume of an NSTAR discharge cathode. They recognized that the conditions were satisfied for the growth of IAT, and that given the past precedent linking high energy ions to IAT, this turbulence might account for the enhanced ion energies needed to explain the observed keeper erosion. Since the IAT is inherently a kinetic effect, however, the authors were unable to check this hypothesis with their fluid-based simulations. In our most recent work, we directly measured the IAT in a 100-A LaB<sub>6</sub> cathode,<sup>25</sup> and we demonstrated at low flow rate a correlation

between the amplitude of IAT turbulence and the growth of a high energy ion tail in the plasma. This observation supported the idea that energetic ions and the IAT are linked in the cathode plume. However, since we did not attempt to explore the mechanism by which energy transfer occurred from the IAT to the ions, we were unable to causally link the processes. The goal of this paper is to explore this causal relationship with an eye toward determining if there is sufficient energy in the measured IAT to create the ion energy tails. In particular, we explore the dominant mechanism by which the IAT can transfer energy to the ions, ion Landau damping, and use experimental measurements in conjunction with one-dimensional modeling to estimate the degree of ion heating that results from the IAT measured in our 100-A cathode.

With this purpose in mind, this work is organized in the following way. In the first section, we outline our experimental setup and diagnostics. In the second section, we establish the correlation between IAT and ion energy through single-point measurements in the cathode plume. In the third section, we present a model to link IAT to the production of high energy ions. In the fourth section, we apply this formalism to a high current case in order to determine if the observed high energy ions can be explained by the measured turbulent spectrum. In the fifth and final section, we discuss mitigation techniques to minimize high energy ion formation.

## II. Experimental Setup

### A. Cathode Assembly

The 100-A cathode assembly (Fig. 1) in our experiment was designed for operation at high current. As reported in detail in Ref. 28, it consists of a graphite tube that houses a LaB<sub>6</sub> insert. A tungsten endplate with an orifice that is 12% the diameter of the cathode tube caps the end. The cathode tube is wrapped with a tantalum coaxial heater that in turn is housed in a graphite keeper. The ratio of the keeper orifice to the keeper diameter is 30%. The setup was installed in the JPL High Current Test Facility, a 2.8 m x 1.3 m cylindrical chamber with vacuum maintained by two cryopumps. The base pressure of this facility was  $\sim 10^{-7}$  T while at the flow rate we examine here, 10 sccm xenon, the background pressure was maintained at  $2.4 \times 10^{-4}$  T. A water-cooled, copper cylinder that was lined with tungsten served as the anode. This was placed  $\sim 3$  cm downstream of the keeper face. While the cathode setup was surrounded by a solenoid capable of generating a magnetic field, for the measurements reported here, no magnetic field was applied.

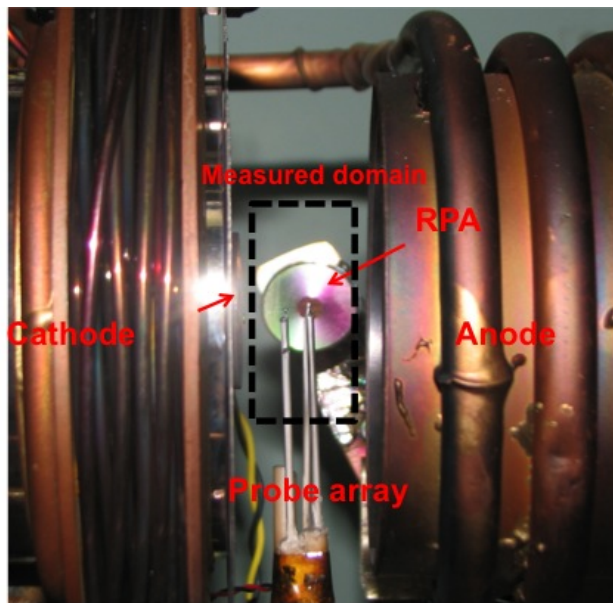


Figure 1: Photo of the 100-A hollow cathode employed in the experiment. The retarding potential analyzer and probe array are indicated. The dotted box marks the region of experimental interrogation with the translating probes.

## B. Diagnostics

In this experiment, we performed measurements to characterize the background plasma, oscillations in the plasma, and ion energies. We discuss in the following the diagnostics we employed to make these measurements and the analysis techniques we used.

### 1. Langmuir Probe

The background plasma density, temperature, and plasma potential were measured with a single Langmuir probe mounted on a two-axis translation system. This allowed for a two-dimensional map of the background plasma parameters of interest in the region between the keeper and the anode. The exposed element of the Langmuir probe was tungsten, 2 mm in length with a diameter of 0.5 mm. The electron temperature was inferred from an exponential fit to the probe IV trace (c.f. Ref. 29), while we employed the thin sheath approximation for cylindrical probes to estimate density,  $n_i = i_{sat} / \left( 0.61 q A_p \sqrt{T_e / m_i} \right)$  where  $A_p$  denotes the probe area. We similarly inferred the plasma potential from the “knee-technique” applied to semi-log plots of the probe IV traces. The measurements reported here were generated from an average of thirty-two probe traces.

### 2. Retarding Potential Analyzer

In order to characterize ion energy, we employed a four-grid, retarding potential analyzer (RPA). The first grid of the RPA was allowed to float; the second, electron-repelling grid was biased negatively with respect to ground; the third grid provided the bias voltage necessary to resolve ion energies; and the fourth grid was negatively biased to suppress secondary electrons. The collector plate was grounded through a 1 MHz resistor, and we inferred the ion current from the drop across this resistor. We generated IV characteristics for this setup by incrementing the RPA bias with a DC power supply at 1 V intervals from 0 to 60 V and measuring the time-averaged current at each voltage. Each scan lasted approximately two minutes.

The IV characteristics from the RPA yield information on the distribution of ion-to-charge energies in the plasma. Without *a priori* knowledge of the fraction of multiply charged states in the plasma, the interpretation of the IV characteristic is problematic. However, provided the plasma is dominated by singly charge species, this diagnostic serves as a proxy for ion energy<sup>30</sup>

$$-\frac{dI}{dV} \approx \beta q^2 f_i(qV), \quad (1)$$

where  $\beta$  is a constant,  $q$  denotes the elementary charge, and  $f_i$  is the ion energy distribution function. Due to the limited space between the keeper and the anode, it was necessary to place the RPA at a distance of 10 cm from the cathode centerline (compared to a plume diameter of  $\sim 2$  cm) with its grids parallel to the plane intersecting the centerline. As such, the RPA was only capable of measuring ion energy in the radial direction.

### 3. Ion saturation and floating probes

To characterize the on-axis, current-driven fluctuations in the cathode plume, we employed the same Langmuir probe outlined in Sec. 1 operated at either floating potential or biased negatively to -30 V with a battery. When negatively biased, the probe collects ion saturation current  $i_{sat}$ , which can be used to estimate fluctuations in plasma potential,  $\phi$ . In particular, for electrostatic modes such as the ion acoustic wave we have  $\phi \approx (T_e/q) \tilde{n}_i / \bar{n}_i$ , where  $\tilde{n}_i$  is the fluctuating density and  $\bar{n}_i$  is the time-averaged density. Assuming ion density scales with the ion saturation current, the electrostatic relationship allows us to relate plasma potential fluctuations to measurements of the ion saturation current:

$$\phi = \frac{T_e \tilde{i}_{sat}}{q \bar{i}_{sat}}. \quad (2)$$

The ion saturation probe is simple to implement, and in light of Eq. 2, it is reliable for estimating fluctuation intensity provided  $\tilde{i}_{sat} \ll \bar{i}_{sat}$ . This probe was the primary diagnostic we employed for our investigation of fluctuations on cathode centerline in Ref. 25, and in order to facilitate comparison with these results, it was the diagnostic we used here to make single-point measurements on cathode centerline.

On the other hand, we found that when we attempted to generate two-dimensional plots of the power spectra with the ion saturation probe, the criterion for the validity of Eq. 2 was violated outside the main beam of the discharge plasma. This was because the plasma density fell off significantly away from the centerline. Noise pickup on the line thus exceeded the measured  $\bar{i}_{sat}$  leading to erroneously large estimates for plasma potential fluctuations. For our two-dimensional maps then, we chose instead to measure fluctuations in the probe floating potential,  $\phi_F$ . Since  $\phi_F = \phi_p - \alpha' T_e$ , where  $\alpha'$  is a constant and  $\phi_p$  is the plasma potential, if we assume  $T_e$  does not fluctuate significantly, oscillations in floating potential can serve as a proxy for fluctuations in plasma potential,  $\tilde{\phi}_F \approx \phi$ .

### III. Experimental Results

#### A. Correlation between fluctuations and energetic ions

The purpose of this section is to reiterate and expand upon the work we reported in Ref. 25 where we demonstrated a correlational link between the amplitude of fluctuations in the cathode plume and the existence of high energy ions. To this end, we reproduce from this reference the power spectra of the fluctuations in plasma potential (as measured with the ion saturation probe noted in Sec. II.3) at a fixed point 0.75 cm downstream of the keeper plane and on the cathode centerline. These are shown in Figs. 2a and 2b as a function of discharge current. To complement these measurements, we more recently determined the ion energy distribution as a function of discharge current with the RPA described in Sec. II.B. These results are shown in Figs. 2c and 2d where we have normalized the distributions in order to achieve a total area under the curve of one.

There are two trends with current illustrated by the RPA traces. At the lowest current,  $I_D = 25$  A, the ion energy distribution is wide with energies up to 50-60 V. As the current increases to  $\sim 65$  A, the distribution decreases in width and the high energy ions disappear. Above 65 A, this trend is reversed and the distribution begins to widen again until 50-60 V ions reappear around  $I_D = 140$  A. At both low and high currents, the appearance of high energy ions is manifested by a long, drawn out tail in the ion distribution function. This is consistent with previous investigations by Friedly et al. who found ion jets formed in the axial direction with increasing current.<sup>5</sup> In order to quantitatively evaluate this effect for our cathode, we have plotted in Fig. 3a the average ion energy,  $\langle E_i \rangle$ , and in Fig. 3b the standard deviation,  $\text{std}(E_i)$ , of ion energy as functions of current. We also have included the cathode discharge voltage,  $V_D$ , for reference. From Fig. 3a we can see that the average ion energy tracks the discharge voltage. This is consistent with the interpretation that many of the ions are born near the anode and therefore gain energy equal to the discharge voltage as they drop from the plume to the grounded collector of the RPA. On the other hand, the appearance of energetic ions exceeding the discharge voltage at both low and high currents (away from the minimum at  $\sim 65$  A) is embodied by the non-monotonic dependence on current of the standard deviation of the ion energy, which we show in Fig. 3b. This similarly explains why  $V_D$  and  $\langle E_i \rangle$  are not one-to-one.

We can see from Figs. 2a and 2b that the amplitude of the fluctuations in the cathode plume exhibit the same qualitative trends as the RPA data. The spectra magnitude initially decreases with current but then begins to increase again between  $I_D = 50$  and 70 A. We quantify this trend explicitly by plotting in Figs. 3a and 3b the total of the power spectra,  $|\tilde{\phi}|_T^2 = \sum_{\omega} \phi_{\omega}^2$ , as a function of discharge current. This reveals that both the average ion energy and the spread in energy distribution directly track the level of fluctuations in the plume. The correlation between fluctuation amplitude is consistent with the qualitative observations we made in Ref. 25.

With this relationship in mind, we next turn to the question of how the fluctuations could be causing the formation of energetic ions. In particular, we concentrate on the high frequency ( $> 200$  kHz) fluctuations exhibited in the spectra shown in Fig. 2a and Fig. 2b, which were identified in Ref. 25 as ion acoustic modes. These oscillations are characterized by a local peak in the power spectra (denoted by the dashed lines in Fig. 2) and a characteristic  $\omega^{-3}$  decay with frequency at high values. We draw attention to these modes because the onset of IAT has been linked both theoretically and experimentally to the formation of high energy ion tails over a wide range of plasma conditions and experiments (c.f. Ref. 17 for a theoretical overview or Ref. 18 for a survey of experimental results). This process can occur for even low level turbulence, i.e. where  $\phi/\phi_p \ll 1$ — an ability that stems from the fact that the acoustic turbulence is propagating and therefore has significant energy associated with the motion of the wave. The qualitative description for how this energy is transferred to the ion tail occurs is as follows. First, the drifting electrons in the plasma give rise to the growth of ion acoustic turbulence through inverse Landau damping (their drift velocity exceeds

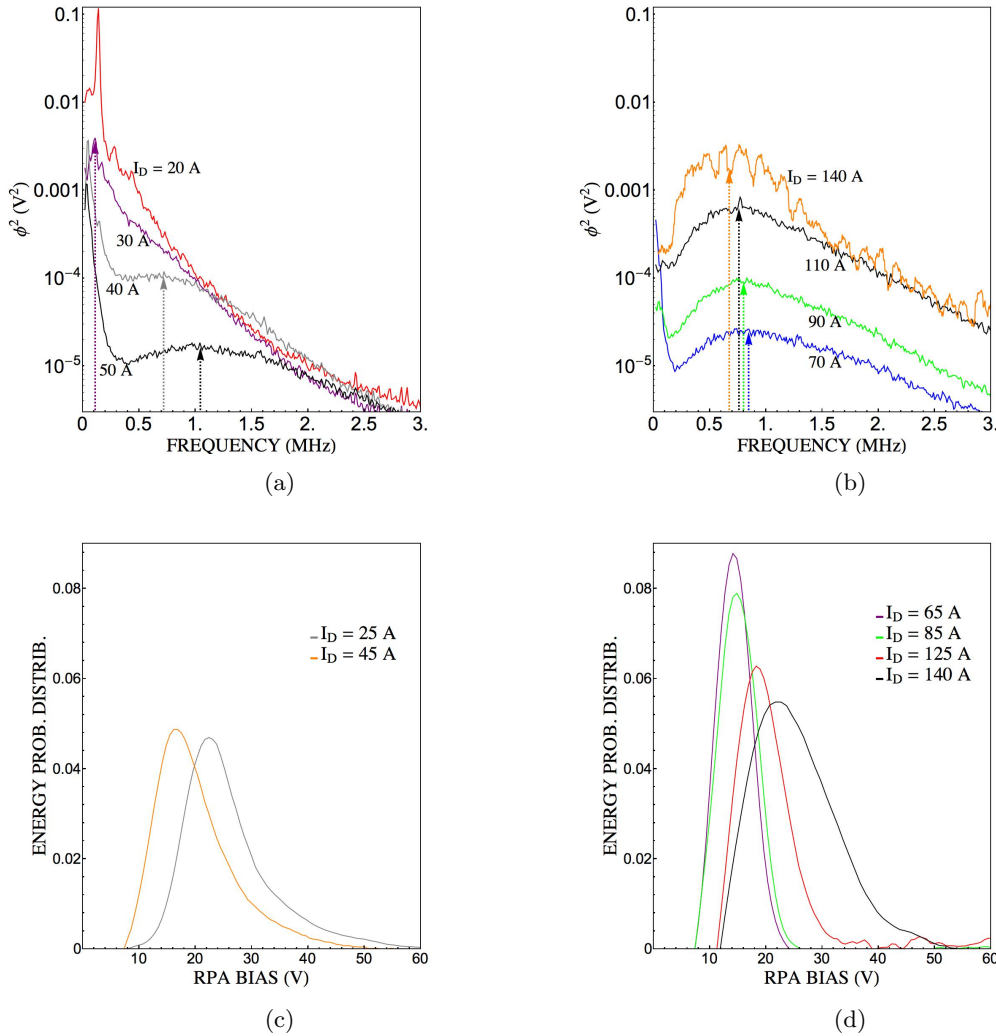


Figure 2: (a) and (b) Power spectra for fluctuations in plasma potential at a position 0.75 cm from the keeper face and on cathode centerline. The resolution is 10 kHz. The maxima in the IAT where it can be resolved is indicated by the dotted arrow. (c) and (d) Radial ion energy distributions as measured with an RPA located 10 cm from the cathode centerline. The flow rate was 10 sccm at all of the reported discharge currents.

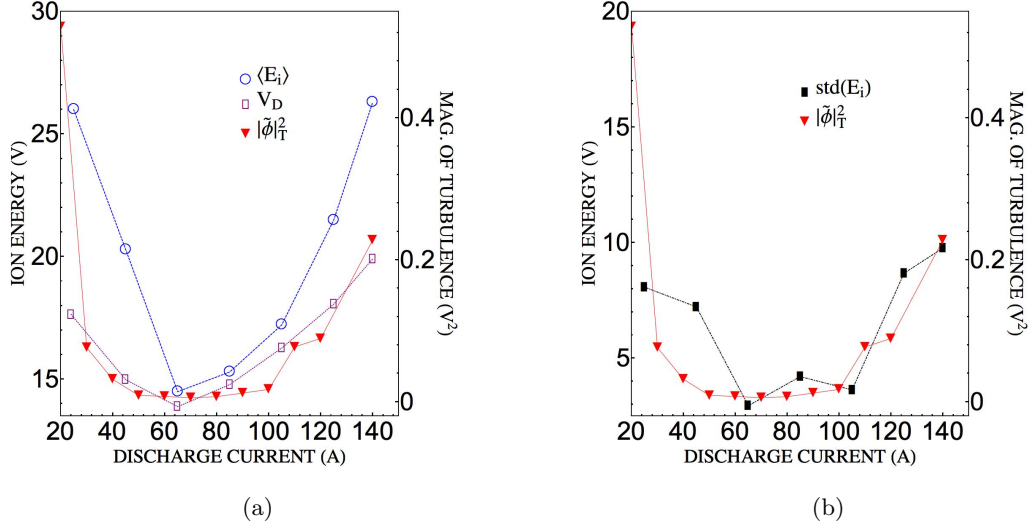


Figure 3: a) Plot of average ion energy, discharge voltage, and total power in the power spectra as functions of discharge current. b) Plot of standard deviation in ion energy and total power in the spectra as functions of discharge current. The flow rate was 10 scfm.

the wave phase velocity). This growth leads to an effective collision frequency that slows down the electron drift, a process which was the subject of our previous investigation into IAT.<sup>25</sup> With the growth of the IAT, ion Landau damping of the wave becomes significant, and ions resonant with the wave phase velocity are heated. Since the wave phase velocity is typically higher than the ion thermal velocity, this process leads to the formation of a high energy ion tail.

In keeping with this interpretation, Fig. 3 shows that above  $I_D = 80$  A, where Fig. 2b indicates the spectra is dominated by the IAT, the total wave energy tracks the increase in thermal spread of the ions. At lower currents, this trend is less evident because a low frequency component at  $\sim 100$  kHz appears in the spectra with an amplitude higher than that exhibited by the IAT peak. This low frequency oscillation is a separate phenomenon than the IAT and is traditionally associated with an ionization mode.<sup>9,25</sup> Ionization-type oscillations have been identified as a possible driver for the production of energetic ions in the cathode plume;<sup>9,16</sup> however, since unlike the IAT they are non-propagating, the mechanism by which ions gain energy from these oscillations requires their amplitudes be commensurate with the energy in the observed ion tail. The power spectra as well as our peak to peak measurements of fluctuations in the plasma suggest that this is not the case for our plasma  $\phi/\phi_p \ll 1$ . The low-frequency oscillations therefore do not have sufficient amplitude to produce energetic ions—though they do have the effect of obscuring the IAT at low currents. This is compounded by the fact that for currents below  $I_D = 65$  A, the location of the peak in the turbulent spectra appears to shift to lower values with decreasing current. At  $I_D = 25$  A, for example, the IAT peak is either coincident or dominated by the narrow ionization peak at 100 kHz, which makes it difficult to isolate the contribution of the IAT to the total power in the oscillations. At low currents, we therefore cannot establish as unambiguous of a link between the power in the IAT and the spread in ion energy as we can for the  $I_D > 80$  A cases. We do note, however, that the IAT is still present at these lower currents as is evidenced by the characteristic slow decrease in the spectra amplitude with frequency.

We thus have showed that at high currents there is a definite correlation between IAT power and the increase in the spread of ion thermal energy. The question of causality remains, however, as to how the turbulence drives tail formation and whether or not the turbulence is sufficiently high in our cathode plume to explain the observed ion tails. In the next section, we present a theoretical formulation for the IAT interaction with the ions in an attempt to answer this question.

## IV. Model for ion tail formation by IAT

We adopt a one-dimensional quasilinear formulation<sup>19</sup> to model the response of the ion distribution function to the acoustic turbulence. In this approach, we assume that the turbulent fluctuations have a random phase. This is consistent with our experimental observation that the acoustic fluctuations in the plasma were not coherent, and it permits us through the quasilinear formalism to treat the interaction of the turbulence with the ion distribution function as a diffusive processes:

$$\frac{\partial f_i}{\partial t} + v \frac{\partial f_i}{\partial x} = \frac{\partial}{\partial v} \left[ D_{QL} \frac{\partial f_i}{\partial v} \right], \quad (3)$$

where  $D_{QL}$  denotes the quasilinear diffusion coefficient. In this model, we neglect the local, steady-state electric field and instead approximate its effect as a net ion drift experienced by the ions,  $v_{di}$ . We similarly neglect collisionality and assume the energy transfer happens on a length scale where the plasma can be approximated as uniform. The form of the diffusion operator is given by<sup>19</sup>

$$D_{QL} = \frac{q^2}{2m_i^2} \sum_k [k\phi_k]^2 \frac{\gamma_k}{(\omega - kv)^2 + \gamma_k^2}, \quad (4)$$

where  $\phi_k$  is the amplitude of the turbulence at the wavenumber  $k$  (related to frequency through the acoustic dispersion relation), and  $\gamma_k$  is the growth rate of the  $k^{th}$  acoustic mode and is given in the laboratory frame by

$$\gamma_k = \left(\frac{\pi}{2}\right)^{1/2} (\omega - kv_{di}) M_e. \quad (5)$$

Here  $v_{di}$  denotes the ion drift velocity, and  $M_e = v_{de}/v_{te}$  is the electron mach number. This term is positive definite and reflects the fact that the growth of the IAT due to electron drift is dominant over potential loss processes. A positive growth is a necessary assumption for the derivation of Eq. 4,<sup>31,32</sup> which is the most expedient form of the diffusion coefficient for numerical calculation. This form, however, does not lend itself to a particularly physically intuitive interpretation for the diffusive process produced by the quasilinear interaction of ions with the waves.

Following the review of quasilinear theory provided in Ref. 33, we can gain more insight by writing the diffusion coefficient as  $D_{QL} = D_R + D_{NR}$  where

$$D_R = \frac{\pi q^2}{2m_i^2} \sum_k [k\phi_k]^2 \delta(\omega - kv) \quad (6)$$

$$D_{NR} = \frac{q^2}{2m_i^2} \sum_k [k\phi_k]^2 \mathcal{P} \left[ \frac{1}{\omega - kv} \right]. \quad (7)$$

Here  $R$  denotes resonant interaction,  $NR$  is non-resonant,  $\delta$  corresponds the Dirac delta function, and  $\mathcal{P}$  is the Principal Value. The resonant term represents the collisionless Landau interaction of the ions with the ions—it is the classically envisioned surfing effect where ions with velocity close to the phase velocity of the wave are subject to collisionless energy exchange with the wave. This term leads to a flattening of the ion distribution for ion velocities near the wave phase velocity,  $\omega/k$ . The second term represents non-resonant diffusion. It reflects the fact that the wave energy of ion acoustic modes is carried by the collective motion of the ions. As a consequence, the more the wave grows, the more energy the bulk, non-resonant ions must have to support it. If the acoustic modes were all coherent, i.e. in phase, this motion would be manifested by a coherent sloshing in the ion distribution function. However, the large number of modes leads to phase mixing and the effect is that the bulk population of the ions can expand in velocity space. This non-resonant term is necessary for a self-consistent, energy-conserving formulation for the wave-particle interaction,<sup>33</sup> and as noted in Ref. 19, it is this parameter that is critical for driving low energy ions into resonant interaction with the wave.

In order to apply Eq. 3 to our cathode plasma, we make the steady-state approximation in the laboratory reference frame. In other the words, the plasma background parameters and levels of turbulence in the cathode plume are constant in time but spatially dependent. This allows us to set  $\partial f_i / \partial t = 0$  in Eq. 3 such

that we have

$$v \frac{\partial f_i}{\partial x} = \frac{\partial}{\partial v} \left[ D_{QL} \frac{\partial f_i}{\partial v} \right]. \quad (8)$$

By knowing the spatial dependence of the turbulence and background plasma parameters, we can solve Eq. 8 to find the steady-state ion distribution as a function of position in the plume. This is consistent with the interpretation of the IAT in the cathode plasma as a convective instability. It is driven unstable when the electron drift velocity exceeds the ion acoustic speed in the plume (c.f. Ref. 27), and then it propagates in the direction of the electron velocity. The turbulence continues to grow spatially as it travels, gaining energy at the expense of the electrons. This process results in a non-uniform spatial distribution of wave turbulence. While ions upstream of the region of strong turbulence are cold, those in the region of turbulence have increased energy that reflects the fact that acoustic modes are largely carried by ion kinetic motion. In the regions of the most intense turbulence, the sloshing of the ion energy associated with carrying the waves pushes some of the ions into resonance with the propagating modes. Resonant diffusion takes over, which sends the ions to even higher velocities. This process forms a high energy tail with ion velocities that can exceed significantly the IAT phase velocity.

To apply Eq. 8 to our cathode plume, we first must measure the spatial distribution of ion acoustic turbulence and then numerically evaluate the expression. We can make a number of simplifying assumptions about the form of  $D_{QL}$  to facilitate this. From our work in Ref. 25, we identified the turbulence as ion acoustic in nature by the stark linearity of the dispersion relation,  $\omega = (c_s + v_{di})k$ . For ion acoustic modes, this linearity holds true provided  $\omega \ll \omega_{pi}$  where  $\omega_{pi}$  denotes the ion plasma frequency. Our measurements in Fig. 2 reveal that the power spectra decreases to noise levels for frequencies well below  $\omega_{pi}$ . Therefore, for our experimental conditions we make the approximation that  $\omega/k = v_\phi = \text{constant}$ . This allows us to re-write Eq. 4 as

$$D_{QL} = \sum_k \frac{\omega' [q\phi_k]^2}{T_e^2} \left[ \left( \frac{\pi}{2} \right)^{1/2} \frac{T_e^2}{m_i^2 (v_\phi - v)^2 + \beta} \right], \quad (9)$$

where  $\omega' = \omega - kv_{di}$  and  $\beta = (\pi/2)(M_e c_s)^2$ . In this expression, the term in the parentheses on the right hand side is independent of wavenumber or amplitude, and the summation can be approximated following Ref. 27 as

$$\frac{\omega' [q\phi_k]^2}{T_e^2} = 2\nu_{AN} \left( \frac{m_e}{m_i} \right)^{1/2}, \quad (10)$$

where  $\nu_{AN}$  is the anomalous collision frequency the IAT induces on the electrons as they gain energy from the electron drift. We thus can write  $D_{QL}$  more compactly as

$$D_{QL} = \frac{T_e^2}{m_i^2} \left( \frac{\pi m_e}{2 m_i} \right)^{1/2} \nu_{AN} \frac{M_e}{(v_\phi - v)^2 + \beta}. \quad (11)$$

This form of the diffusion term lends itself to the physical interpretation we have provided for the interaction of the IAT with the ions. The waves grow at the expense of the electrons, which is represented by the anomalous collision frequency  $\nu_{AN}$ . This energy is then in part transferred to the ions, which is embodied by the appearance of  $\nu_{AN}$  in the ion diffusion equation. Indeed, at the resonant condition  $v = v_\phi$ , we find that

$$D_{QL} \propto \frac{T_e}{m_i} \nu_{AN}. \quad (12)$$

This is consistent with the classical interpretation of the diffusion operator as a Markovian process:  $D \sim \langle \Delta v \rangle^2 / \Delta \tau_{ac}$  where  $\tau_{ac} = 1/\nu_{AN}$  is the autocorrelation time, the time between randomizing kicks in energy, and  $\langle \Delta v \rangle^2 \sim c_s^2$  is an incremental change in energy produced by this kick. In this case, the change in energy scales with the acoustic energy of the mode.

Finally, in order to facilitate numerical calculation, we normalize Eq. 8 and the diffusion operator according to the convention  $V = v/v_{ti(0)}$ ,  $X = x/\lambda_i$ , and  $\bar{f}_i \rightarrow f_i v_{ti(0)}$  where  $v_{ti(0)}$  denotes the initial, cold

thermal velocity of the ion distribution in the region upstream of turbulence and  $\lambda_i$  is the ion Debye length. We thus can write the kinetic equation in one dimension as

$$V \frac{\partial \bar{f}_i}{\partial X} = \frac{\partial}{\partial V} \left[ \bar{D}_{QL} \frac{\partial \bar{f}_i}{\partial V} \right], \quad (13)$$

where

$$\bar{D}_{QL} = \alpha^2 \frac{\nu_{AN}}{\omega_{pe}} \left( \frac{\pi}{2} \right)^{1/2} \frac{M_e}{(V_\phi - V)^2 + \bar{\beta}}. \quad (14)$$

Here  $\alpha = T_e/T_{i0}$  and  $\bar{\beta} = \alpha (\pi/2) M_e^2$ . In this simplified form, we can determine how the ion distribution function depends on position provided we know the total power in the ion acoustic turbulence (as embodied by  $\nu_{AN}$ ), the electron Mach number,  $M_e$ , at the region of interest, and the background plasma parameters.

## V. Investigation of tail formation at high current condition

In order to apply the formalism from the previous section to our cathode, we examine the unambiguous operating point at 140 A and 10 sccm where high energy ions are present and IAT is clearly the dominant oscillation. The spatial dependence of the plasma parameters for this condition is shown in Fig. 4 along with a photo of the cathode in operation. From these measurements, we see that the plasma potential exhibits a minimum at the centerline which then increases in the radial direction. The plasma temperature and density, on the other hand, decrease monotonically with radius. The electron temperature is non-monotonic along the cathode centerline and exhibits a peak at a position downstream of the keeper.

In Fig. 4e we show the spatial dependence of the integrated turbulence  $|\tilde{\phi}|_T^2$  as measured with the floating probe described in Sec. II.B. The fluctuations exhibit a region of low turbulence immediately near the keeper at centerline and then reach a peak downstream. The location of this peak is near the maximum in electron temperature, which is consistent with the interpretation that the growth of the IAT leads to an effective collision frequency for the electrons.<sup>25</sup> Indeed, the monotonic increase in temperature with axial position cannot be explained without invoking such an anomalous collision frequency in our cathode.<sup>26</sup> Evidence of anomalous collision frequency due to IAT similarly has been argued in other electric propulsion hollow cathodes of different size and operating condition.<sup>21,22</sup>

We can use the measurements from Fig. 4 to estimate an average Mach number on the centerline. Assuming the electrons carry the current in the plasma, the axial component of the current density is given by  $j_z = qn_e(r, z)u_{e(z)}(r, z)$ , where  $u_{e(z)}$  is the drift of electrons in the axial direction. Integrating the current density over an area at fixed axial position yields the total discharge current:

$$I_D = 2\pi \int_0^{r_{max}} j_z r dr = q2\pi \int_0^{r_{max}} n_e(r, z)u_{e(z)}(r, z)r dr, \quad (15)$$

where we have assumed the density goes to zero at  $r_{max}$ . We note from Fig. 4c that the density is highly concentrated near the cathode centerline. We therefore simplify the above integral by making the approximation

$$\int_0^{r_{max}} n_e(r, z)u_{e(z)}(r, z)r dr = \bar{u}_e(z) \int_0^{r_{max}} n_e(r, z)r dr, \quad (16)$$

where  $\bar{u}_{e(z)}(z)$  is an average value for the electron velocity at centerline. Substituting this relation into Eq. 15, we find

$$\bar{u}_e(z) = \frac{I_D}{q2\pi \int_0^{r_{max}} n_e(r, z)r dr}. \quad (17)$$

We use the centerline value of  $T_e$  from Fig. 4d to estimate the electron thermal velocity,  $v_e = \sqrt{T_e/m_e}$ , and we divide Eq. 17 by this velocity to yield the electron Mach number on the centerline as a function of axial position. This result is shown in Fig. 5a where we can see the parameter is approximately constant over our experimentally integrated domain with a value of  $M_e \approx 0.15$ .

With this last element of experimentally measured data, we now have sufficient information to numerically solve Eq. 13. We do this for an ion distribution evolving spatially along the centerline of the cathode from

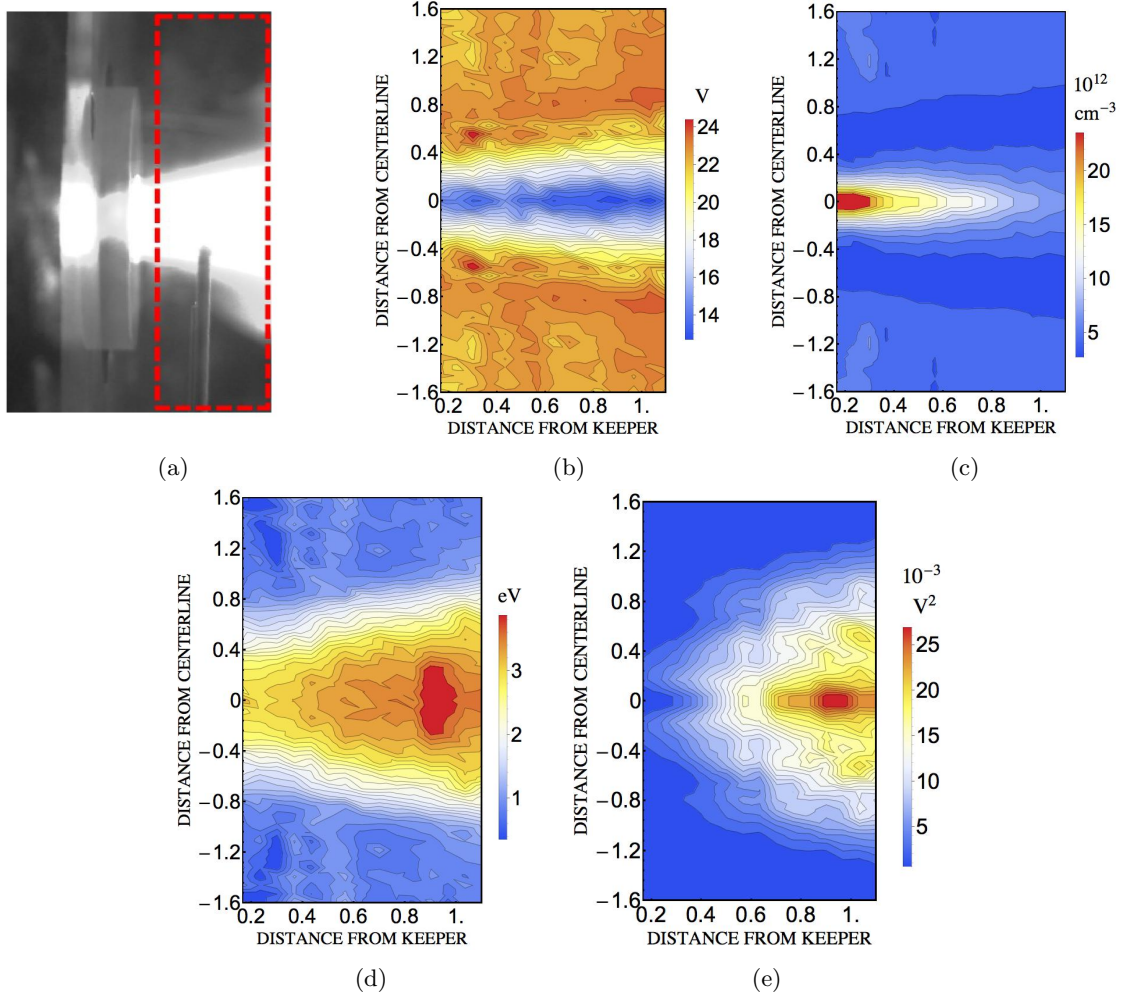


Figure 4: Spatial dependence of steady-steady plasma parameters in the near plume for 140 A and 10 scm. (a) Photo of cathode plume where the outlined rectangle corresponds to the location of plasma measurements; (b) plasma potential; (c) plasma density; (d) electron temperature; (e) sum of the power spectra of floating potential fluctuations as a function of position. The radial and axial positions have been normalized by  $r_k$ , the keeper radius and the resolution is  $0.07r_k$ .

$z = 0.3r_k$  to  $z = 0.75r_k$  ( $r_k$  denotes the keeper radius), where the turbulent amplitude begins to saturate according to Fig. 5b. Along this domain, the assumption of a uniform background plasma that facilitated the derivation Eq. 13 is approximately valid: the plasma density and electron temperature both change less than 30%. We therefore assume a constant density and an electron temperature of  $T_e = 3$  eV. We similarly use the average value of  $M_e = 0.15$  indicated by Fig. 5a. As for the parameter  $\nu_{AN}/\omega_{pe}$  over this domain, we relate it to the turbulent amplitude with the expression derived in Ref. 27 and later implemented by us in Ref. 25:

$$\frac{\nu_{AN}}{\omega_{pe}} = \sum_k \frac{[q\phi_k(\omega)]^2}{T_e^2}. \quad (18)$$

Since we do not have direct measurements of the ion temperature, we perform our simulations for a range of values of  $\alpha$ .

We show in Fig. 5b the spatial dependence of the anomalous collision frequency on cathode centerline as dictated by substituting our measurements from Fig. 4d and Fig. 4e into Eq. 18. With this known profile and our other experimental measurements, we can see that all of the coefficients in Eq. 13 are known. We therefore can solve for  $\bar{f}_i$  as a function of  $V$  and  $X$  by numerically evaluating this relation with a simple

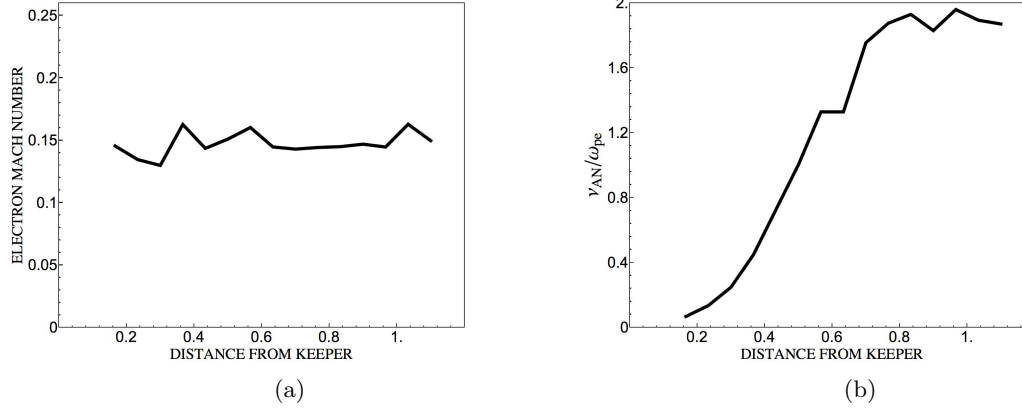


Figure 5: a) Estimate for electron Mach number along channel centerline. b) Estimate for the parameter  $\nu_{AN}/\omega_{pe}$  along the cathode centerline.

finite differencing scheme. To this end, we employ 200 discrete values of normalized velocity from  $V = 0$  to  $V = 35$  and a spatial step of  $\Delta X = 1$ . At each step, the ion drift is re-calculated from  $\bar{f}_i$  and used to determine the phase velocity of the wave in the laboratory frame,  $V_\phi$ . For the initial condition at  $r = 0.3r_k$ , we assume the ions are cold and drifting with  $v_{di} = 2500$  m/s, which is consistent with our findings from Ref. 25 where we inferred the ion drift velocity along the centerline from the measured dispersion relation.

Numerically integrating Eq. 13 with our finite differencing scheme yields the spatial evolution of the ion distribution for the sample case of  $\alpha = 30$  shown in Fig. 6a. The initial distribution function at the upstream edge of the turbulence is a drifting Maxwellian with normalized velocity  $V = 8$ . At  $z = 0.38r_k$ , we can see a tail begins to form at the resonant velocity ( $V_\phi = \sqrt{\alpha} + V_{di} = 15$ ) of the waves in the laboratory frame. With increasing wave energy, as embodied by  $\nu_{AN}/\omega_{pe}$  in Fig. 5b, the non-resonant diffusion pushes more ions up to this wave phase velocity. The result is an even larger spreading in velocity space. In order to relate this change in normalized velocity distribution to the ion energy distributions we measured with an RPA, we convert the unnormalized ion velocity  $v = Vv_{ti}$  to kinetic energy,  $m_i v^2/2$ , and add the discharge voltage  $V_D = 20$  V to account for the potential drop from the plasma to the RPA collector ground. The result of this transformation is shown in Fig. 6b where we can see that the impact of the IAT is to produce an energetic ion tail. The shape of this tail is consistent with previous experimental results performed by Friedly et. al<sup>5</sup> where jets of high energy ions were observed in RPA traces axially downstream of the cathode. We also note the magnitude of the energy in the tail is comparable to the actual measurements from our RPA (Fig. 2d).

We have performed a parametric analysis to investigate the impact of the parameter  $\alpha$  on the energy in the ion tail. The chosen range,  $\alpha = 15 - 90$ , is physically plausible for our cathode plasma. For values that are too low,  $\alpha < 10$ , ion Landau damping may prevent the wave from ever being driven unstable,<sup>27</sup> which is not the case for our plasma. And for the upper bound,  $\alpha = 90$ , the corresponding ion temperature is 0.03 eV. This is a plausible lower bound for ion temperature given that the cathode insert temperature for our cathode is  $\sim 1500$  C.<sup>26</sup> We show the results of our simulations at  $z = 0.72r_k$  in Fig. 6c over this range of  $\alpha$  where it is immediately evident that the influence of this parameter is small. Provided the actual value of  $\alpha$  in the experiment falls within our specified range, this result suggests that the IAT heating should have a noticeable impact on the ion energy

With this in mind, we note that even though there is sufficient ion energy in the simulated distribution to explain our experimental results, there are significant differences in the shapes. In particular, the ion tail from the simulations is not thermalized like the ion distribution functions indicated by our RPA measurements from Fig. 6b. This stems from the fact that collisions were not incorporated into Eq. 13. This is not an unrealistic assumption in the region of intense turbulence where the growth rate satisfies  $\gamma_\omega/\nu_{ii} = (\omega/\nu_{ii}) M_E \gg 1$ ; however, due to space constraints, it was necessary to place our RPA at a position 10 cm off axis from the cathode plume. This was well beyond the region of intense turbulence such that there was a transit time during which the ions could have had time to thermalize. The disparity between experiment and simulation therefore may be the result of thermalization redistributing the energy introduced by the waves.

The differences between measurement and simulation may also be attributed to the fact that we simulated

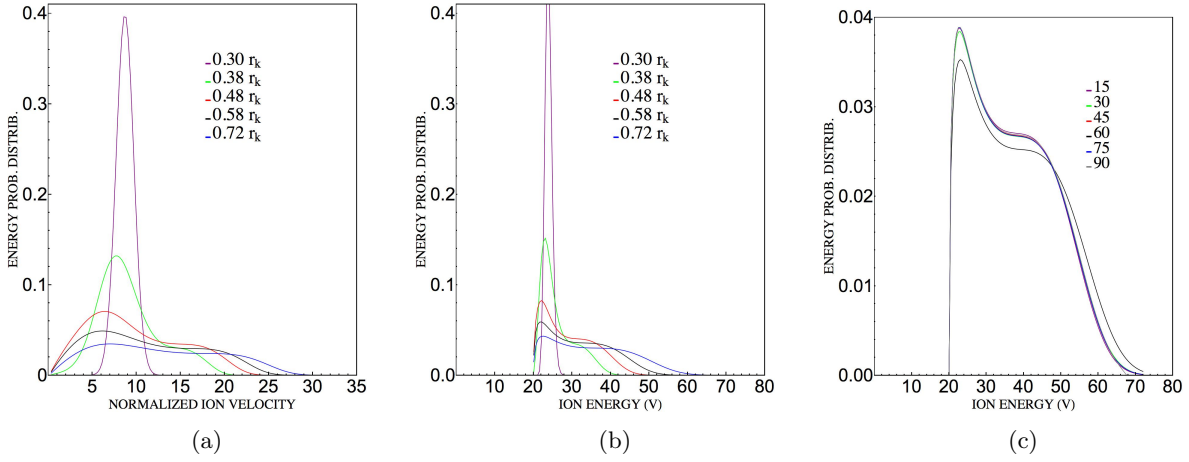


Figure 6: Evolution of the ion distribution function as a function of position in the cathode plume according to Eq. 13. a) The normalized distribution as a function of normalized velocity on centerline. b) The same distribution function as (a) expressed in terms of ion energy that an RPA would measure assuming a 20 V drop from cathode plume to ground. c) The ion energy distribution function at position  $z = 0.72r_k$  as a function of  $\alpha$ .

the ion axial distribution while we measured the radial ion energy distribution. In particular, while there is no question experimentally that an ion tail does form in the radial direction, it is possible that the energy for the ion tail we estimate with our axial formation may be different than that exhibited in the radial direction. Ishihara et al., for example, found that when there are wave components that are oblique with respect to the electron drift, greater heating in the radial direction can occur than observed in the axial.<sup>34</sup> On the other hand, the review work done in Ref. 17 showed that IAT heating of ions in the direction perpendicular to the electron drift (radial for our case) is comparable to that exhibited in the parallel direction. Self-consistently evaluating the radial heating for our cathode plasma is beyond the scope of this work given the two-dimensionally inherent to the radial components of the propagating waves (Fig. 4e). Our estimates for heating in the axial direction therefore must serve as a proxy to explain the effects we observe experimentally.

With this in mind, our work here has served the purpose of demonstrating that there is a mechanism for the IAT to produce an energetic ion tail and that there is sufficient energy in the IAT to explain the experimentally observed ion energies. These observations and our correlational results shown in Fig. 3 support the argument that the relationship between the IAT and the formation of the high ion energy is causal in our cathode plasma. This result of course does not preclude the existence of other mechanisms for energetic ion production—most notably the production of ion energies by the large voltage swings that occur in strong plume mode.<sup>9,16</sup> However, given that our cathode does not appear to be operating in this regime, the IAT process should be the dominant effect. Assuming this is the case, in the following section we discuss mitigation techniques that could be employed to reduce energetic ion production in the plume.

## VI. Mitigation techniques

Provided that the source of high energy ions in our high current hollow cathode is dependent on the IAT, reducing the turbulence may mitigate energetic ion production. We discuss three techniques for achieving this end in the following section: identifying the right operating point, neutral injection, and seeding the propellant with lighter particles.

### A. Changing operating point

A parametric investigation from single point measurements has revealed that increasing the gas flow rate reduces the amplitude of turbulence at a fixed current (c.f. Fig. 7 in Ref. 25). This suggests that it may be possible to move the location of the minimum in turbulent amplitude exhibited in Fig. 3 by changing the flow rate. Provided we can control the location of this minimum, the correlation between IAT amplitude and

energetic production provides a simple operational guideline that could be implemented to mitigate energetic ion production for a desired output current: adjust the flow rate until the minimum in IAT is achieved. Alternatively, it is evident from Eq. 13 that the energy exchange of the waves with the ions is driven by the electron Mach number as well as the degree of anisotropy between electron and ion temperatures,  $\alpha$ . By switching to larger cathode orifices, it may be possible to change these parameters in such a way as to eliminate the IAT.<sup>35</sup> A trade off in moving to this parameter space, however, is that the cathode may be pushed into plume mode. To date, we have investigated IAT amplitude as a function of pressure, but we have not yet measured the ion distribution function as it responds to flow rate and varying orifice size. That will be the subject of immediate follow on work.

## B. Neutral injection

Previous experimental investigations into high energy ion production in the cathode plume have indicated that neutral injection from an external sources in the cathode plume will reduce the level of energetic ions.<sup>11, 13</sup> While this may be in part due to enhanced charge-exchange collisions, Mikellides et al. suggested that neutral injection may be collisionally damping the ion acoustic turbulence and thereby leading to the reduction of energetic ions. In support of this thesis, Goebel et al. experimentally demonstrated that oscillations in the cathode plume are in fact damped by neutral injection.<sup>36</sup> This collisional-damping effect is also consistent with our experimental findings correlating the IAT and the formation of the ion tail. Ultimately, isolating the exact reason for the mitigation of the energetic ions is difficult in light of the fact that previous neutral gas injection experiments were performed with nozzles that spread gas throughout the entire plume. By selectively injecting gas into a small, spatially compact region in the gas, however, we may be able to rule out the large effects of charge exchange collisions and instead focus on the impact of the local damping of the IAT on the measured ion energy distribution function.

## C. Seeding with light particles

If IAT is the leading cause of energetic ion production in our hollow cathode, a viable method for suppressing this mechanism could be to seed the propellant with a small fraction of lighter gas particles such as helium. Given the greater spread in thermal velocity that these lighter particles have, the minority species dominates the ion collisionless heating process—effectively damping out the IAT from Landau resonances before the heavier particles can be heated. The effect of introducing lighter species particles on the damping of IAT has been demonstrated both theoretically and experimentally,<sup>37</sup> and there is some experimental evidence that introducing nitrogen into the gas mix of hollow cathodes helped mitigate erosion effects. In particular, Garner et al. found that by seeding the discharge cathode of a 30-cm ion engine with 0.5 – 2% nitrogen, the erosion of elements of the discharge chamber located downstream of the cathode was significantly reduced.<sup>38</sup> The role of the nitrogen in reducing erosion was purported to be due to the formation of nitrogen and nitride layers on the discharge elements; however, it is also possible that seeding the gas with this lower mass particle may have reduced the high energy ions by suppressing the IAT.

## VII. Discussion

The results from the above investigation offer a self-consistent picture for the formation of energetic ions in the hollow cathode plume. This process can be viewed as one evolving in space since the background parameters and turbulence levels in the plasma are at steady state. First, when the conditions for growth are satisfied, the electron drift drives the IAT unstable. This leads to an increase in the amplitude of the IAT in the direction of electron drift. As the IAT grows, the kinetic energy of the ions propagating the mode also increases. This is because ion acoustic modes are largely carried by ion motion. The ion sloshing due to the wave growth pushes some of the particles into resonance with the IAT phase velocity, and it is the resulting resonant diffusion of these particles that leads to the formation of a high-energy tail. We have showed that the amplitude of the waves is sufficiently high in the cathode plume to allow for the formation of ion energy tails commensurate with those we measured with an RPA. This process occurs even though the relative amplitude of the turbulence is low compared to the background plasma potential and thermal energy,  $T_e$ .

With these results in mind, we draw attention to the fact that the above discussion applies to the case where IAT is the dominant oscillation in the plasma. On the other hand, there have been a number of

previous experiments where the cathodes seemingly were operated in plume mode, which is characterized by very large peak-peak, low-frequency fluctuations in plasma potential. This swing can be more than sufficient at these operating conditions to explain the energetic ions observed in these cathodes.<sup>9,16</sup> We also note that the above model we employed is still subject to a number of simplifying assumptions. In particular, we have largely avoided the questions of nonlinearity, collisionality, and non-uniformity of the plasma. These can only be addressed by adding higher order terms into our formulation, Eq. 13. Identifying the correct way to implement these effects into the model is non-trivial—particularly given the wide range of theories surrounding nonlinear turbulent effects in IAT (c.f. Ref. 17). Moving to this next degree of complexity does not appear to be necessary, however, as the quasilinear approximation has been able to demonstrate that the IAT does have sufficient energy to produce the observed RPA traces. As a final note, the mitigation techniques we have outlined above are applicable provided the IAT is in fact the dominant mechanism for the production of high energy ions. They will work in different measure, and investigating the efficacy of these methods is paramount for moving forward in designing new cathode systems capable of achieving long-life, high-current operation.

## VIII. Conclusion

In this study, we have addressed the role of IAT in the formation of energetic ions in a high current hollow cathode. We have showed that for a fixed flow rate and varying discharge current that the amplitude of the IAT is correlated with the formation of energetic ions. This is an unsurprising result given the large body of work associating these modes with the growth of energetic ion tails. In an attempt to move beyond a correlational relationship and establish causality, we have modeled the interaction of the ion distribution function in the cathode with the IAT by means of an experimentally-informed, quasilinear diffusion equation. We have showed that when taking into account both resonant and non-resonant diffusion and our experimental conditions, it is possible to explain the appearance of a high energy ion tail in the cathode plume. The shape of the resulting distribution function in the axial direction was consistent with previous experimental measurements of high current hollow cathodes where the ion energy was monitored at a position axially downstream.<sup>5</sup> On the other hand, our modeled shape for the ion energy distribution did not completely recreate the measurements we made with a radially-oriented RPA. We have conjectured that this discrepancy may be explained by collisional thermalization of the distribution that we neglected in our formulation.

Given the correlation between IAT and energetic ions and the existence of a mechanism to causally link the two, there are a number of mitigation methods that may be employed to reduce the ion tails. We have outlined three of these processes: tailoring the cathode operating point and/or geometry to minimize IAT, injecting neutrals to collisionally damp the IAT, and seeding the xenon with a much lighter gas to collisionlessly damp the IAT. A systematic investigation of these mitigation techniques will be the focus of the final phase of the two-year NASA Research and Technology Demonstration (R&TD) grant awarded to examine high energy ion formation in high-current hollow cathodes. The results of these future studies, guided by the work in this paper, will be critical for extending the life of high current cathodes to the requisite levels called for by the next generation of high-power EP missions.

## Acknowledgments

The research described in this paper was carried out by the Jet Propulsion Laboratory, California Institute of Technology, under a contract with the National Aeronautics and Space Administration and funded through the internal Research and Technology Development program.

## References

<sup>1</sup>Polk, J., Anderson, J., Brophy, J., Rawlin, V., Patterson, M., Sovey, J., and Hamley, J., “An overview of the results from an 8200 hour wear test of the NSTAR ion thruster,” *35th AIAA/ASME/SAE/ASEE Joint Propulsion Conference, June 20 - 24, 1999, Los Angeles, CA. AIAA-99-2446*.

<sup>2</sup>Sengupta, A., Brophy, J. R., and Goodfellow, K. D., “Status of the extended life test of the Deep Space 1 flight spare ion engine after 30,352 hours of operation,” *39th AIAA/ASME/SAE/ASEE Joint Propulsion Conference, July 20-23, 2003 Huntsville, AL. AIAA-03-4558*.

<sup>3</sup>Mikellides, I. G. and Katz, I., “Wear Mechanisms in Electron Sources for Ion Propulsion, I: Neutralizer Hollow Cathode,”

*Journal of Propulsion and Power*, Vol. 24, No. 4, 2008, pp. 855–865.

<sup>4</sup>Brophy, J. and Garner, C., “Tests of High-Current Cathodes for Ion Engines,” *24th AIAA/ASME/SAE/ASEE Joint Propulsion Conference, July 11-13, 1988. Boston, MA. AIAA-88-2193*.

<sup>5</sup>Friedly, V. and Wilbur, P., “High current hollow cathode phenomena,” *Journal of Propulsion and Power*, Vol. 8, No. 3, 2008, pp. 635–643.

<sup>6</sup>Williams, G., Smith, T., Domonkos, M., Gallimore, A., and Drake, R., “Laser-induced fluorescence characterization of ions emitted from hollow cathodes,” *Plasma Science, IEEE Transactions on*, Vol. 28, No. 5, 2000, pp. 1664–1675.

<sup>7</sup>Williams, G., Domonkos, M. T., and Chavez, J. M., “Measurement of doubly charged ions in ion thruster plumes,” *27th International Electric Propulsion Conference, Oct. 14-19, 2001. Pasadena, CA. IEPC-01-310*.

<sup>8</sup>Foster, J. E. and Patterson, M. J., “Downstream Ion Energy Distributions in a Hollow Cathode Ring Cusp Discharge,” *Journal of Propulsion and Power*, Vol. 21, No. 1, Jan. 2005, pp. 144–151.

<sup>9</sup>Goebel, D. M., Jameson, K. K., Katz, I., and Mikellides, I. G., “Potential fluctuations and energetic ion production in hollow cathode discharges,” *Physics of Plasmas*, Vol. 14, No. 10, 2007.

<sup>10</sup>Farnell, C. C., Williams, J. D., and Farnell, C. C., “Comparison of hollow cathode discharge plasma configurations,” *Plasma Sources Science and Technology*, Vol. 20, No. 2, 2011.

<sup>11</sup>Chu, E., Goebel, D. M., and Wirz, R. E., “Reduction of Energetic Ion Production in Hollow Cathodes by External Gas Injection,” *Journal of Propulsion and Power*, Vol. 29, No. 5, June 2013, pp. 1155–1163.

<sup>12</sup>Latham, P., Pearce, A., and Bond, R., “Erosion processes in the UK-25 ion thruster,” *22nd International Electric Propulsion Conference, Oct, 1991, Viareggio, Italy, IEPC-91-096*.

<sup>13</sup>Kameyama, I., “Effects of Neutral Density on Energetic Ions Produced Near High-Current Hollow Cathodes,” Tech. Rep. NASA CR-204154, Oct. 1997.

<sup>14</sup>Katz, I., Mikellides, I. G., Goebel, D. M., Jameson, K. K., and Johnson, L., “Production of high energy ions near an ion thruster discharge hollow cathode,” *42nd AIAA/ASME/SAE/ASEE Joint Propulsion Conference and Exhibit, July 9-12, 2006. Sacramento, CA. AIAA-2006-4485*.

<sup>15</sup>Gallimore, A. and Rovey, J., “Erosion Processes of the Discharge Cathode Assembly of Ring-Cusp Gridded Ion Thrusters,” *Journal of Propulsion and Power*, Vol. 23, No. 6, 2007, pp. 1271–1278.

<sup>16</sup>Mikellides, I. G., Katz, I., Goebel, D. M., Jameson, K., and Polk, J., “Wear Mechanisms in Electron Sources for Ion Propulsion, II: Discharge Hollow Cathode,” *Journal of Propulsion and Power*, Vol. 24, No. 4, 2008, pp. 866–879.

<sup>17</sup>Bychenkov, V., Silin, V., and Uryupin, S., “Ion-acoustic turbulence and anomalous transport,” *Physics Reports*, Vol. 164, No. 3, 1988, pp. 119 – 215.

<sup>18</sup>de Kluiver, H., Perepelkin, N., and Hirose, A., “Experimental results on current-driven turbulence in plasmas - a survey,” *Physics Reports*, Vol. 199, No. 6, 1991, pp. 281 – 381.

<sup>19</sup>Ishihara, O. and Hirose, A., “Quasilinear Mechanism of High-Energy Ion-Tail Formation in the Ion-Acoustic Instability,” *Physical Review Letters*, Vol. 46, No. 12, 1981.

<sup>20</sup>Guyot, M. and Hollenstein, C., “Experiments on Potential Gradients in a Current-Carrying Plasma, 1: Potential Structures,” *Soviet Journal of Atomic Energy*, Vol. 26, No. 6, 1967.

<sup>21</sup>Mikellides, I. G., Katz, I., Goebel, D. M., and Polk, J. E., “Hollow cathode theory and experiment II: A two-dimensional theoretical model of the emitter region,” *Journal of Applied Physics*, Vol. 98, No. 11, 2005, pp. 113303.

<sup>22</sup>Mikellides, I. G., Katz, I., Goebel, D. M., and Jameson, K. K., “Evidence of nonclassical plasma transport in hollow cathodes for electric propulsion,” *Journal of Applied Physics*, Vol. 101, No. 6, 2007, pp. 063301.

<sup>23</sup>Goebel, D., Jameson, K., Katz, I., and Mikellides, I., “Energetic Ion Production and Keeper Erosion in Hollow Cathode Discharges,” *29th International Electric Propulsion Conference, Oct. 31-Nov. 4, Princeton, NJ. IEPC-2005-266*.

<sup>24</sup>Goebel, D. M., Jameson, K. K., Watkins, R. M., Katz, I., and Mikellides, I. G., “Hollow cathode theory and experiment I. Plasma characterization using fast miniature scanning probes,” *Journal of Applied Physics*, Vol. 98, No. 113302.

<sup>25</sup>Jorns, B., Mikellides, I., and Goebel, D., “Temporal Fluctuations in a 100-A LaB6 Hollow Cathode,” *33rd International Electric Propulsion Conference, Oct. 6 - 10, 2013 Washington D.C. IEPC-2013-385*.

<sup>26</sup>Mikellides, I. G., Goebel, D. M., Jorns, B. A., Polk, J., and Guerrero, P., “Numerical Simulation of the Partially-ionized Gas in a 100-A LaB6 Hollow Cathode,” *33rd International Electric Propulsion Conference, October 6 - 10, 2013, Washington, D.C. IEPC-2007-124*.

<sup>27</sup>Sagdeev, R. and Galeev, A., *Nonlinear plasma theory*, Frontiers in physics, W. A. Benjamin, 1969.

<sup>28</sup>Chu, E. and Goebel, D. M., “High-Current Lanthanum Hexaboride Hollow Cathode for 10-to-50-kW Hall Thrusters,” *Plasma Science, IEEE Transactions on*, Vol. 40, No. 9, 2012, pp. 2133–2144.

<sup>29</sup>Chen, F. F., “Langmuir probe diagnostics,” *Mini-Course on Plasma Diagnostics, IEEE-ICOPS Meeting, Jeju, Korea, 2003*.

<sup>30</sup>Hutchinson, I., *Principles of Plasma Diagnostics*, Cambridge University Press, 2005.

<sup>31</sup>Burns, T., “Revision and Test of the Quasilinear Theory,” *Physics of Fluids*, Vol. 15, No. 4, 1972, pp. 610.

<sup>32</sup>Vahala, G. and Montgomery, D., “Discrete spectra and damped waves in quasilinear theory,” *Journal of Plasma Physics*, Vol. 4, 12 1970, pp. 677–691.

<sup>33</sup>Stix, T., *Waves in Plasmas*, AIP, New York, 1992.

<sup>34</sup>Ishihara, O., “High-energy ion tail formation in the ion-acoustic instability—A Three-dimensional quasilinear approach,” *Physics of Fluids*, Vol. 26, No. 1, 1983, pp. 100.

<sup>35</sup>Mikellides, I. G., Katz, I., and Goebel, D. M., “Numerical Simulation of the Hollow Cathode Discharge Plasma Dynamics,” *29th International Electric Propulsion Conference, Oct. 31-Nov. 4, Princeton, NJ. IEPC-2005-200*.

<sup>36</sup>Goebel, D., Jameson, K., Katz, I., and Mikellides, I., “Plasma Potential Behavior and Plume Mode Transitions in Hollow Cathode Discharges,” *30th International Electric Propulsion Conference, Sept. 17-20, 2007. Florence, Italy. IEPC-2007-277*.

<sup>37</sup>Alexeff, I., Jones, W. D., and Montgomery, D., "Controlled Landau Damping of Ion-Acoustic Waves," *Phys. Rev. Lett.*, Vol. 19, Aug 1967, pp. 422-425.

<sup>38</sup>Garner, C., Brophy, J., Pless, L., and Barnett, J., "Effect of Nitrogen on Xenon Ion Engine Erosion," *21st International Electric Propulsion Conference, July 18-20, 1990. Orlando, FL. AIAA-90-2951.*